Sequence-Mandated, Distinct Assembly of Giant Molecules

Wei Zhang, Xinlin Lu, Jialin Mao, Chih-Hao Hsu, Gaoyan Mu, Mingjun Huang, Qingyun Guo, Hao Liu, Chrys Wesdemiotis, Tao Li, Wen-Bin Zhang,* Yiwen Li,* and Stephen Z. D. Cheng*

Abstract: *Although controlling the primary structure of synthetic polymers is itself a great challenge, the potential of sequence control for tailoring hierarchical structures remains to be exploited, especially in the creation of new and unconventional phases. A series of model amphiphilic chain-like giant molecules was designed and synthesized by interconnecting both hydrophobic and hydrophilic molecular nanoparticles in precisely defined sequence and composition to investigate their sequence-dependent phase structures. Not only compositional variation changed the self-assembled supramolecular phases, but also specific sequences induce unconventional phase formation, including Frank–Kasper phases. The formation mechanism was attributed to the conformational change driven by the collective hydrogen bonding and the sequence-mandated topology of the molecules. These results show that sequence control in synthetic polymers can have a dramatic impact on polymer properties and self-assembly.*

Natural polymers, such as deoxyribonucleic acids, ribonucleic acid, and proteins, accomplish highly sophisticated functions to sustain life with a small set of simple building blocks arranged in precisely defined composition, length, sequence, and stereochemistry. Their properties and performances are in fact mandated by the information encoded in polymer sequences. The importance of sequence has also been demonstrated in some bio-resembling polymers, such as peptides, peptoids, and nucleic acids,[1] which inspired the next generation sequence-controlled synthetic polymers. Recently, with contributions from Lutz, Du Prez, Haddleton, Liu, and others, tremendous progress has been made on the synthetic methods.[2] Although the synthesis of sequence-controlled polymers at a similar level of precision to natural polymers is an enormous endeavor by itself,[3] it remains to be demonstrated how sequence could dictate molecular topology and assembly toward different structures and functions in synthetic polymers.[2c, 4] While assembly of most synthetic macromolecules is driven by interaction of monomers,[5] the minute differences between individual monomers are often insufficient to discriminate assembly pathways. Thus, precisely controlled collective and cooperative interactions have been increasingly recognized as the key process to form hierarchical structures with feature sizes of only a few nanometers.[6] In this case, oligomers/polymers with nanosized macromonomers[7] is an effective approach to build phase-separated nanostructures with the most significant impact of sequence.

The imposing challenge that we are facing is not only to achieve a macromolecule with precisely defined sequences and sizes, but also to design and control their self-assembled structures and develop desired properties. Recent advances of click chemistry and other efficient transformations allow scientists to achieve macromolecules with high structural precision and controlled heterogeneity. On the other hand, the supramolecular structures are modularly assembled from a set of building blocks and thus the topology and interaction of each building block are critically important to the final assembled structures. They, in turn, must be accurately determined by the composition and sequence of the macromolecule. Aiming at such an enormous task, we begin by rationally designing a series of model amphiphilic giant molecules (so-called "giant" relative to their small-molecule counterparts)[8] for the study of sequence-phase relationships and the role of sequences in the formation unconventional phases in soft matters.[9] More specifically, these giant molecules here refer to precise macromolecules build-up by molecular nanoparticle building blocks. We have previously investigated the effects of composition and topology on the self-assembly of giant molecules.[4b, 6c, 9d, 10] However, the importance of sequence has not been systematically explored in terms of their impact on phase formation.

Herein, the rational design of model compounds was based on linearly-like configured, monodisperse giant molecules with consecutively connected polyhedral oligomeric

[*] W. Zhang, X. Lu, C. Hsu, G. Mu, M. Huang, Q. Guo, H. Liu,
Prof. C. Wesdemiotis, Prof. S. Z. D. Cheng
Department of Polymer Science
College of Polymer Science and Polymer Engineering
The University of Akron, Akron, OH 44325-3909 (USA)
E-mail: scheng@uakron.edu

J. Mao, Prof. C. Wesdemiotis
Department of Chemistry
The University of Akron, Akron, OH 44325-3601 (USA)

T. Li
X-ray Science Division, Advanced Photon Source
Argonne National Laboratory, Argonne, IL 60439 (USA)
and
Department of Chemistry and Biochemistry
Northern Illinois University, DeKalb, IL 60115 (USA)

Prof. W. B. Zhang
Key Laboratory of Polymer Chemistry and Physics of the Ministry of
Education, College of Chemistry and Molecular Engineering, Center
for Soft Matter Science and Engineering
Peking University, Beijing 100871 (China)
E-mail: wenbin@pku.edu.cn

Prof. Y. Li
College of Polymer Science and Engineering, State Key Laboratory of
Polymer Materials Engineering, Sichuan University
Chengdu 610065 (China)
E-mail: ywli@scu.edu.cn

Supporting information for this article (detailed synthetic routes,
characterization methods, samples preparation, and other data) can
be found under:
https://doi.org/10.1002/anie.201709354.

silsesquioxane (POSS) molecular nanoparticles (NP). For simplicity, only two types of repeating units were employed: the hydrophobic BPOSS (ca. 1 kDa with 7 *sec*-butyl groups) and the hydrophilic DPOSS (ca. 1.5 kDa with 14 hydroxy

Figure 1. A) Chain-like giant molecules with precisely controlled sequences and compositions built up by both hydrophilic and hydrophobic (D and B) POSS NPs. *x* and *y* are the number of BPOSS nanoparticles on the left and right side of the DPOSS in the linear-like giant molecules. *n* is the total number of the BPOSS NPs. B) The general synthetic strategy for these molecules.

groups). Each POSS NP is a building block that can be viewed as a macromonomer or a precise block of polymer. The detailed molecular structures are illustrated in Figure 1. We believe that the collective interaction between different macromonomers could enable efficient construction of novel nanostructures, thus the attachment of large-sized NPs will make the sequence effect even more pronounced. This series of amphiphilic giant molecules could thus serve as a good platform to understand the sequence effect in synthetic macromolecules. From a chemistry point of view, tuning exact number of nanoparticles with precise chemical structures to build the giant molecules eliminates the batch to batch variations in conventional polymers due to polydispersity.[11] We could also precisely manipulate their connecting sequence to achieve different sequence isomers in a way similar to playing with building blocks. From a physics point of view, they have large enough immiscibility to induce nanophase separation between different NPs. The thermodynamic driving force is the strong collective hydrogen bonding formed by dense hydroxy groups on the peripheries of DPOSS cages among the giant molecules. The hydrophobic BPOSS NPs are nanophase separated from DPOSS NPs ($\chi >$ 0.3, see the Supporting Information for calculations[12]). Owing to the incompatibility of these two kinds of nanoparticles, BPOSS NPs tend to stay away from DPOSS NPs.[10a] Notably, their selective interactions dominate the formation of building blocks via macromolecular packing arrangements and become the most important factor in determining their assembled structures. The building blocks are thus constructed by a core of DPOSS NPs aggregated together and covered with a thick shell formed by BPOSS NPs. It should be

noted that stereochemistry refers another important parameter in natural polymers. However, this factor is not the focus of the current study and thus are not discussed further herein.

There are two dimensions to tune their structures and properties, namely composition and sequence. In detail, the local conformation of individual giant molecules would be relatively extended in the tails when $x = 0$ in Figure 1. We speculate that as the number of hydrophobic BPOSS (n) increases, it becomes increasingly difficult to force the BPOSS NPs to line up within the cross-sectional area of one DPOSS NP owing to the progressively elevated entropic penalty. This would possibly lead to phase structures evolving from LAM→HEX→BCC, like many asymmetric block copolymers. When $x \neq 0$ in Figure 1, the local conformation of individual molecules would be in distinct folded states with respect to the DPOSS NP in the tails by specific design of DPOSS position in the chain sequence. From left to right along the horizontal lines (as x increases) in Figure 1, the tail conformation changes from non-folded to asymmetric, and finally to symmetric/close-to-symmetric folded conformations with changing the NP sequence at designated composition. We hypothesize that the sequence effect in the molecules could induce folded conformation driven by the collective hydrogen bonding among the hydrophilic molecular NPs and influenced by the sequence-mandated topology of the hydrophobic NPs, finally determining the interfacial areas of the two phases at designate composition. This would result in different "fan-angles", "cone-angles" of the whole molecules, which could affect the aggregation numbers or even possibly induce phase transformations.

These monodisperse giant molecules (with molecular weights as high as > 7000) exhibit single lines that are accurate to the atomic level based on matrix assisted laser desorption/ionization-time of flight (MALDI-TOF) mass spectra as shown in Figure 2. The general synthetic illustration is shown in Figure 1 B and the detailed routes and characterizations (^{1}H, ^{13}C NMR and other MS spectra) are outlined in the Supporting Information.

These amphiphilic giant molecules exhibit versatile ordered supramolecular phases with sub-10 nm feature sizes typically after thermal annealing for 2 h at about 150 °C. When the BPOSS cage does not crystallize, multiple hydrophilic DPOSS cages start aggregating together via the collective hydrogen bonding that forms one nanophase and
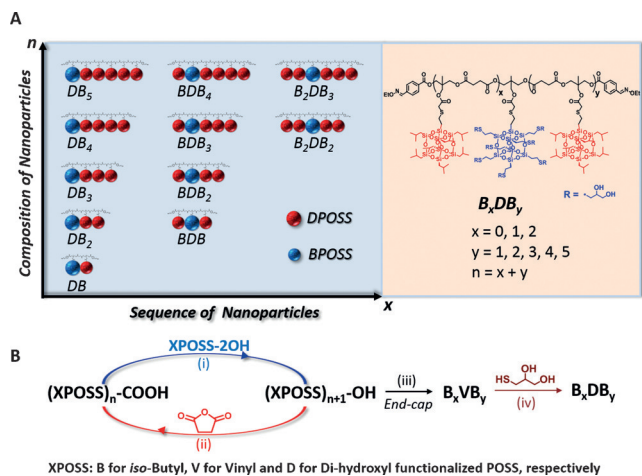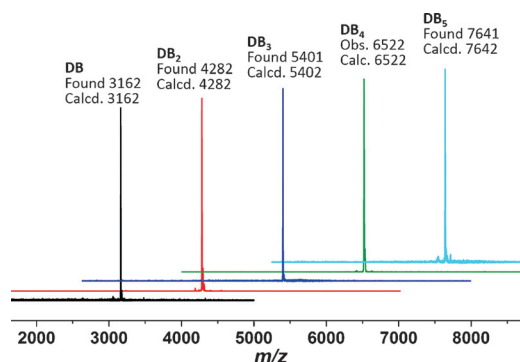

Figure 2. MALDI-TOF spectra of DB$_n$ ($n = 1$–5). All of the samples show peaks of [M·Ag]$^+$ corresponding to the calculated molecular weights.
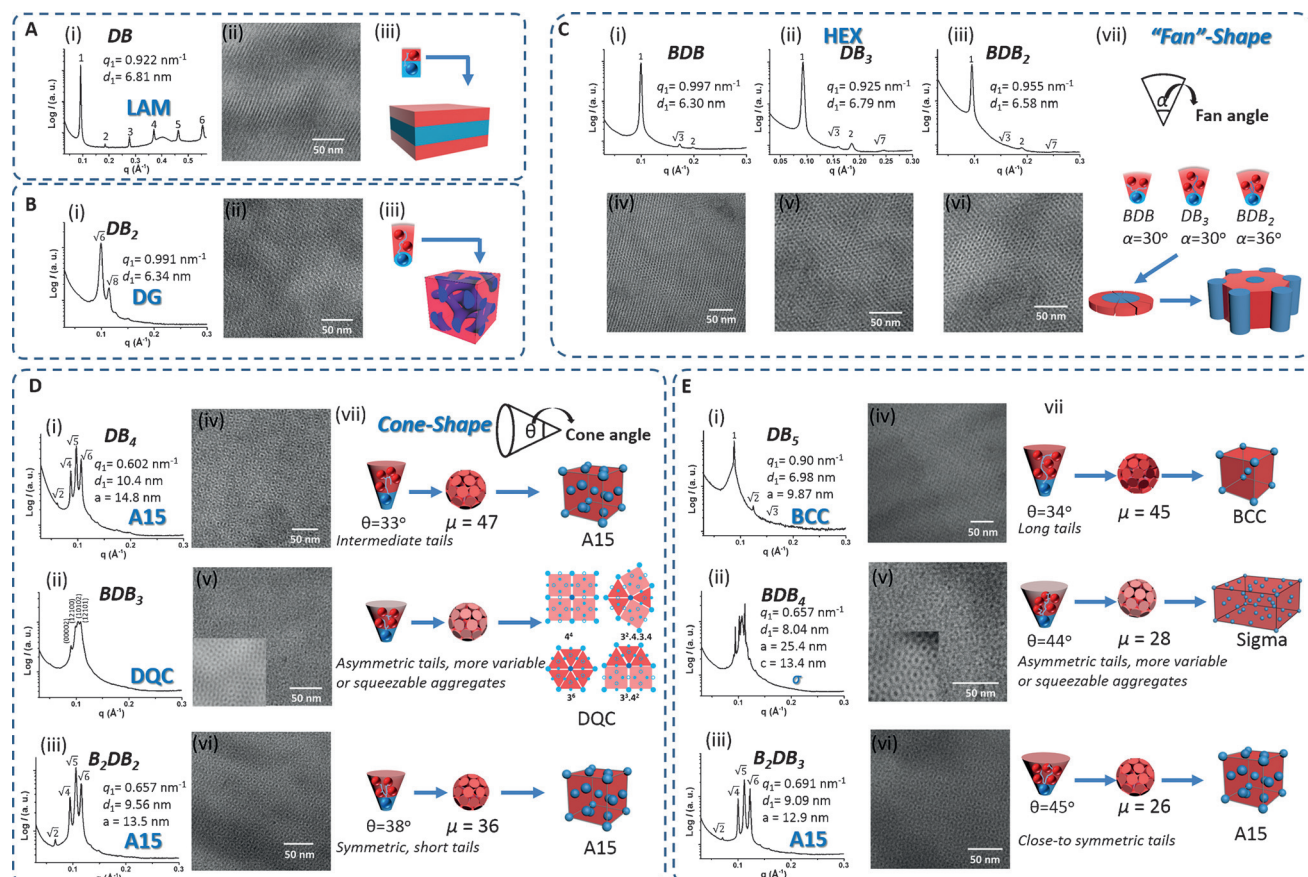
Figure 3. SAXS patterns, TEM images, and packing models of giant molecules. A) DB forms a LAM phase. B) DB_2 forms a DG phase. C) BDB, DB_3, and BDB_2 adopt fan-shapes and form HEX phases. D) DB_4, BDB_3, and B_2DB_2 adopt cone-shapes and form A15, DQC and A15 phases, respectively. The inset in (v) is the Fourier filtered image. E) DB_5, BDB_4, and B_2DB_3 adopt cone shapes and form BCC, σ and A15 phases, respectively. The inset in (v) is the Fourier filtered image.

push out the rest hydrophobic BPOSS cages to organize into the other phase.

For DB ($n=1$, $x=0$ in Figure 1), it has no sequence isomer. With more or less commensurate size of the two NPs, an alternating layered structure is expected from this molecule. A small-angle X-ray scattering (SAXS) pattern shows multiple peaks of equal q interval, indicating a lamellar (LAM) lattice with layer spacing of 6.81 nm (Figure 3 A(i)). The lamellar structure is also confirmed by the bright field (BF) TEM image in real space (Figure 3 A(ii)).

For DB_2 ($n=2$, $x=0$), a double gyroid (DG) lattice (with a space group of $Ia\bar{3}d$) can be observed based on characteristic q ratio of diffractions of $\sqrt{6}:\sqrt{8}$ in the SAXS pattern (Figure 3 B(i)). In this DG lattice, two BPOSS cages are sequentially and linearly tethered on the DPOSS cage, and the aggregated DPOSS cages via collective hydrogen bonding are imbedded in the BPOSS matrix (Figure 3 B(ii)). However, by moving the DPOSS cage to the second position ($x=1$), the sequence isomer BDB adopts a symmetric folded conformation with unbalanced interface between DPOSS and two BPOSS cages. The SAXS pattern of BDB exhibits scattering vector q ratio of $1:\sqrt{3}:\sqrt{4}$ in Figure 3 C(i), indicating the formation of a hexagonal packed cylindrical (HEX) structure. The real space image observed via BF TEM is shown in Figure 3 C(iv). The average fan angles (α) for each molecule

can be estimated in BDB to be about 30° (Table 1; for detailed calculations, see the Supporting Information).

DB_3 ($n=3$, $x=0$) and its isomer BDB_2 ($n=3$, $x=1$) both exhibit HEX structures (Figure 3 C), yet with different lattice sizes (6.79 and 6.58 nm). Among them, each BDB_2 molecule possesses an asymmetric folded conformation in the assembly,

Table 1: Supramolecular structure analysis of giant molecules.

Molecules	Phase	a [nm][a]	r [nm][b]	μ[c]	α or θ[d]
DB	LAM	6.81	–	–	–
DB_2	DG	6.34	–	–	–
BDB	HEX	6.30	3.64	12	30°
DB_3	HEX	6.79	3.92	12	30°
BDB_2	HEX	6.58	3.80	10	36°
DB_4	A15	14.8	4.59	47	33°
BDB_3	DQC	–	–	–	–
B_2DB_2	A15	13.5	4.19	36	38°
DB_5	BCC	9.87	4.86	45	34°
BDB_4	σ	$25.4^2 \times 13.4$	4.09	28	43.6°
B_2DB_3	A15	12.9	4.00	26	45.2°

[a] Dimensions of the phase: lamellar periodicities, inter-column distances of HEX lattice, lattice dimensions of A15, BCC and σ lattices. [b] dimensions of the motif: radiuses plates in HEX, radiuses of spheres in A15, BCC and σ lattices. [c] number of molecules per spherical building block. [d] fan-angle (α) or cone angle (θ).

while DB_3 does not. Therefore, BDB_2 sample contains a larger fan angle and a lower number of molecules per unit length of the cylinder (10 molecules per DPOSS cage thickness, $\alpha \approx 36°$, Table 1, see the Supporting Information for calculation) compared to the DB_3 (12 molecules per DPOSS cage thickness, $\alpha \approx 30°$), which leads to a smaller lattice size of BDB_2 (6.58 nm) than that of DB_3 (6.79 nm, Table 1).

When the BPOSS cage number exceeds three, the incommensurate volumes between DPOSS and BPOSS cages become increasingly large. This may cause the molecules to form a cone-like shape to accommodate this volume difference; the shape of building blocks must be spherical, leading to further assemble into spherical phases. For example, in traditional diblock copolymer systems, BCC structures are usually observed in cases with spherical building blocks. Interestingly enough, however, DB_4 ($n = 4$, $x = 0$) shows an unanticipated Frank–Kasper (F-K) A15 phase (space group $Pm\bar{3}n$ (O_h^3)) with characteristic q ratio of $\sqrt{2}:\sqrt{4}:\sqrt{5}:\sqrt{6}$ in the SAXS patterns as shown in Figure 3 D(i) and a representative tiling number of 4^4 in the BF TEM images along the [001] zone in Figure 3 D(iv).[10a] Note that F-K phases were originally found in many metal alloys that possess topological close packing combining the Frank lattice (distorted icosahedral with coordination number, CN, of 12) and the Kasper polyhedra (with CN of 14, 15, or 16).[13] Some F-K phases were also recently found in soft materials, such as dendrimers, block copolymers etc.[9a,b,d,14] The A15 is one of three basic phases in the series of F-K phases with two types of slightly different sizes of the spherical building blocks in a ratio of 1:3.[15] Its crystal structure (space group $Pm\bar{3}n$ (O_h^3)) involves both the Frank lattice (CN: 12) and the Kasper polyhedra (CN: 14). Although the F-K phase formation mechanism remains elusive in soft matters, the formation of a F-K A15 phase is probably due to the deformable and squishable nature and volume exchange of the spherical building blocks. Thermodynamically, the A15 phase possesses a better sphericity of building blocks,[16] and a lower interfacial tension with higher stretching energy compared with those in BCC.[17] When we move the DPOSS cage from the chain end to the second position, BDB_3 ($n = 4$, $x = 1$) starts to adopt the folded conformation. However, with the asymmetric number of BPOSS cages on both side of the DPOSS cage, this might generate surface defects at the spherical building blocks of BDB_3. In this case, the supramolecular structure of BDB_3 is identified to be a dodecagonal quasicrystal (DQC), as illustrated by the characteristic SAXS pattern (the 00002, 12100, 10102, and 12101 diffractions in Figure 3 D(ii)). More than one representative tiling patterns of $3^2.4.3.4$, $3^3.4^2$, 4^4 and 3^6 could be observed in the BF TEM image in Figure 3 D(v), illustrating that the structure losses the translational symmetry along the $a*b*$-plane.[9d,14a] For B_2DB_2 ($n = 4$, $x = 2$), the sequence change resulted in shorter but symmetric BPOSS tails, and it forms an A15 phase again. In this A15 structure, each molecule adopts the folded conformation in the assembly and possesses a larger cone angle (ca. 38°, Table 1; see the Supporting Information for calculations), a smaller average number of molecules in one spherical building block ($\mu = 36$, Table 1, see the Supporting Information for calcu-

lations) and thus, a smaller lattice spacing ($a = 13.5$ nm) compared to the DB_4 case (with a cone angle 33°, $\mu = 47$, $a = 14.8$ nm).

By further increasing the number of BPOSS cages to five, the long BPOSS tail length in DB_5 ($n = 5$, $x = 0$) would impose higher entropy penalty if it remains in an extended chain conformation. It is found to form a BCC structures (space group of $Im3m$) with $a = 9.86$ nm as shown in Figure 3 E(i) and (iv). While for BDB_4 ($n = 5$, $x = 1$) with asymmetric folded conformation, the resulting SAXS pattern shows a set of peaks that can be assigned as a σ lattice (space group $P4_2/mnm$) with tetragonal unit cell parameters $a = b = 25.4$ nm, $c = 13.4$ nm as shown in Figure 3 E(ii) and (v). In the σ phase, there are two spherical building blocks with different sizes in equal number ratio, which are packed in a way combining the Frank Lattice (CN: 12) and two types of Kasper polyhedra (CN: 14 and 15).[9a,14b] For B_2DB_3 ($n = 5$, $x = 2$) with close to symmetric conformation and shortened BPOSS chain length (only 3), it possesses an A15 lattice with $a = 12.9$ nm (Figure 3 E). Detailed supramolecular lattice parameters for all these self-assembled structures are listed in Table 1.

How can these experimental observations and the general implications be understood? If we examine the first left column in Figure 1, it is evident that this series of samples only represent the compositional variation without alternating the sequences. With increasing the volume fraction of the BPOSS cages from about 1/2 to 5/6, the supramolecular structure evolves from LAM to DG to HEX to A15 and finally, to BCC phases. This phase sequence with the volume fraction has been reported experimentally,[9d] and predicted theoretically.[18] It is very interesting that phase structures also change with identical volume fraction but distinct sequences. For example, in the first line of DB_5 series in Figure 1, with moving the DPOSS cage from $x = 0$ to $x = 3$, the phase structure changes from BCC to σ and to A15 phases (also see the second row of DB_4 series). The rationale for the phase structure changes in this series of chain-like giant molecules is probably due to the effect of overall macromolecular topologies dominated by the folded conformation. Namely, the sequence variation first transcripts into the disparity in macromolecular topology, which, in turn, translates into the distinct molecular packing, leading to different ordered supramolecular lattices. The incommensurate cross-section areas between hydrophilic and hydrophobic components lead to curved interfaces to stabilize the supramolecular lattices. Furthermore, the deformability and squeezability of the spherical building blocks are also mainly attributed to the rearrangement and relocation of the BPOSS cages after the folded conformation and the confined packing of each giant molecule in the assembly. Note that no matter how these BPOSS cages pack in the thick shell of the spherical aggregates, their density must remain constant (measured to be about 1.2 g cm^{-3}). In comparison to previous cases with F-K phases formed by block copolymers, our results highlight the ability to tune phase structures with precise composition and sequence.

In summary, we have specifically designed a library of chain-like giant molecules with precisely defined sequences and compositions. This system contains a pair of interactions:

collective hydrogen bonding and nanophase separation, namely, the hydrogen bonding and hydrophilic/hydrophobic interactions. Starting from DPOSS nanoparticle located at one end of the chain and increasing the number of hydrophobic BPOSS, these chain-like giant molecules create lattices from LAM, DG, to HEX, F-K A15, and BCC structures. By moving the DPOSS nanoparticle toward the center of the chain, a series of sequence isomers with identical composition was prepared. The distinct locations of DPOSS mandate the folded conformation of giant molecules into different conformations, which further results in different supramolecular lattices including F-K A15, σ as well as DQC structures. As designed, the molecules with symmetric/asymmetric folded conformation significantly affect the ordered lattice structure formations within this window of unconventional phases. This work has demonstrated the importance of primary structure, especially molecular sequence, in mandating molecular topologies to affect their self-assembly behaviors in these linear-like POSS-based giant molecules. We envision that the building blocks are not limited as POSS nanoparticles and could also include other functional motifs (for example, optical, electric, magnetic). Tremendous interesting materials could be constructed by incorporating more complicated precise sequence with multiple cooperative/competing interactions or functionalities. Inspired by this work and general rule in giant molecules to systematically develop macromolecules with precision at molecular-weight scale as well as at the sequence scale, a new field of synthetic polymeric materials could be opening.

Acknowledgements

Conflict of interest

The authors declare no conflict of interest.

[1] a) J. Sun, A. A. Teran, X. Liao, N. P. Balsara, R. N. Zuckermann, *J. Am. Chem. Soc.* **2013**, *135*, 14119–14124; b) C. Leng, H. G. Buss, R. A. Segalman, Z. Chen, *Langmuir* **2015**, *31*, 9306–9311; c) Y. Suzuki, G. Cardone, D. Restrepo, P. D. Zavattieri, T. S. Baker, F. A. Tezcan, *Nature* **2016**, *533*, 369–373; d) R. V. Thaner, Y. Kim, T. I. N. G. Li, R. J. Macfarlane, S. T. Nguyen, M. Olvera de la Cruz, C. A. Mirkin, *Nano Lett.* **2015**, *15*, 5545–5551; e) C.-L. Chen, R. N. Zuckermann, J. J. DeYoreo, *ACS Nano* **2016**, *10*, 5314–5320; f) P. A. Korevaar, C. J. Newcomb, E. W. Meijer, S. I. Stupp, *J. Am. Chem. Soc.* **2014**, *136*, 8540–8543.

[2] a) J.-F. Lutz, M. Ouchi, D. R. Liu, M. Sawamoto, *Science* **2013**, *341*, 1238149; b) N. Badi, J.-F. Lutz, *Chem. Soc. Rev.* **2009**, *38*, 3383–3390; c) R. K. Roy, A. Meszynska, C. Laure, L. Charles, C. Verchin, J.-F. Lutz, *Nat. Commun.* **2015**, *6*, 7237; d) S. Martens, J. Van den Begin, A. Madder, F. E. Du Prez, P. Espeel, *J. Am. Chem. Soc.* **2016**, *138*, 14182–14185; e) N. G. Engelis, A. Anastasaki, G. Nurumbetov, N. P. Truong, V. Nikolaou, A. Shegiwal, M. R. Whittaker, T. P. Davis, D. M. Haddleton, *Nat. Chem.* **2017**, *9*, 171–178; f) D. M. Rosenbaum, D. R. Liu, *J. Am. Chem. Soc.* **2003**, *125*, 13924–13925.

[3] a) A. Al Ouahabi, L. Charles, J.-F. Lutz, *J. Am. Chem. Soc.* **2015**, *137*, 5629–5635; b) J. C. Barnes, D. J. C. Ehrlich, A. X. Gao, F. A. Leibfarth, Y. Jiang, E. Zhou, T. F. Jamison, J. A. Johnson, *Nat. Chem.* **2015**, *7*, 810–815; c) Y. Hibi, M. Ouchi, M. Sawamoto, *Nat. Commun.* **2016**, *7*, 11064; d) W. R. Gutekunst, C. J. Hawker, *J. Am. Chem. Soc.* **2015**, *137*, 8038–8041; e) S. C. Solleder, M. A. R. Meier, *Angew. Chem. Int. Ed.* **2014**, *53*, 711–714; *Angew. Chem.* **2014**, *126*, 729–732; f) B. Lewandowski, G. De Bo, J. W. Ward, M. Papmeyer, S. Kuschel, M. J. Aldegunde, P. M. E. Gramlich, D. Heckmann, S. M. Goldup, D. M. D'Souza, A. E. Fernandes, D. A. Leigh, *Science* **2013**, *339*, 189–193; g) F. A. Leibfarth, J. A. Johnson, T. F. Jamison, *Proc. Natl. Acad. Sci. USA* **2015**, *112*, 10617–10622.

[4] a) U. S. Gunay, B. E. Petit, D. Karamessini, A. Al Ouahabi, J.-A. Amalian, C. Chendo, M. Bouquey, D. Gigmes, L. Charles, J.-F. Lutz, *Chem* **2016**, *1*, 114–126; b) W. Zhang, M. Huang, H. Su, S. Zhang, K. Yue, X.-H. Dong, X. Li, H. Liu, S. Zhang, C. Wesdemiotis, B. Lotz, W.-B. Zhang, Y. Li, S. Z. D. Cheng, *ACS Cent. Sci.* **2016**, *2*, 48–54; c) M. Porel, D. N. Thornlow, N. N. Phan, C. A. Alabi, *Nat. Chem.* **2016**, *8*, 590–596.

[5] H.-C. Kim, S.-M. Park, W. D. Hinsberg, *Chem. Rev.* **2010**, *110*, 146–177.

[6] a) J.-F. Lutz, J.-M. Lehn, E. W. Meijer, K. Matyjaszewski, *Nat. Rev. Mater.* **2016**, *1*, 16024; b) W. Zhang, Y. Chu, G. Mu, S. A. Eghtesadi, Y. Liu, Z. Zhou, X. Lu, M. A. Kashfipour, R. S. Lillard, K. Yue, T. Liu, S. Z. D. Cheng, *Macromolecules* **2017**, *50*, 5042–5050; c) Y. Chu, W. Zhang, X. Lu, G. Mu, B. Zhang, Y. Li, S. Z. D. Cheng, T. Liu, *Chem. Commun.* **2016**, *52*, 8687–8690.

[7] S. Alexandris, A. Franczyk, G. Papamokos, B. Marciniec, K. Matyjaszewski, K. Koynov, M. Mezger, G. Floudas, *Macromolecules* **2015**, *48*, 3376–3385.

[8] M. J. Boerakker, J. M. Hannink, P. H. H. Bomans, P. M. Frederik, R. J. M. Nolte, E. M. Meijer, N. A. J. M. Sommerdijk, *Angew. Chem. Int. Ed.* **2002**, *41*, 4239–4241; *Angew. Chem.* **2002**, *114*, 4413–4415.

[9] a) G. Ungar, Y. Liu, X. Zeng, V. Percec, W.-D. Cho, *Science* **2003**, *299*, 1208–1211; b) K. Kim, M. W. Schulze, A. Arora, R. M. Lewis, M. A. Hillmyer, K. D. Dorfman, F. S. Bates, *Science* **2017**, *356*, 520–523; c) M. Peterca, M. R. Imam, S. D. Hudson, B. E. Partridge, D. Sahoo, P. A. Heiney, M. L. Klein, V. Percec, *ACS Nano* **2016**, *10*, 10480–10488; d) K. Yue, M. Huang, R. L. Marson, J. He, J. Huang, Z. Zhou, J. Wang, C. Liu, X. Yan, K. Wu, Z. Guo, H. Liu, W. Zhang, P. Ni, C. Wesdemiotis, W.-B. Zhang, S. C. Glotzer, S. Z. D. Cheng, *Proc. Natl. Acad. Sci. USA* **2016**, *113*, 14195–14200.

[10] a) M. Huang, C.-H. Hsu, J. Wang, S. Mei, X. Dong, Y. Li, M. Li, H. Liu, W. Zhang, T. Aida, W.-B. Zhang, K. Yue, S. Z. D. Cheng, *Science* **2015**, *348*, 424–428; b) X. Feng, R. Zhang, Y. Li, Y.-l. Hong, D. Guo, K. Lang, K.-Y. Wu, M. Huang, J. Mao, C. Wesdemiotis, Y. Nishiyama, W. Zhang, W. Zhang, T. Miyoshi, T. Li, S. Z. D. Cheng, *ACS Cent. Sci.* **2017**, *3*, 860–867; c) H. Liu, J. Luo, W. Shan, D. Guo, J. Wang, C.-H. Hsu, M. Huang, W. Zhang, B. Lotz, W.-B. Zhang, T. Liu, K. Yue, S. Z. D. Cheng, *ACS Nano* **2016**, *10*, 6585–6596; d) X.-M. Wang, Y. Shao, J. Xu, X. Jin, R.-

H. Shen, P.-F. Jin, D.-W. Shen, J. Wang, W. Li, J. He, P. Ni, W.-B. Zhang, *Macromolecules* **2017**, *50*, 3943–3953.

[11] J. M. Widin, A. K. Schmitt, A. L. Schmitt, K. Im, M. K. Mahanthappa, *J. Am. Chem. Soc.* **2012**, *134*, 3834–3844.

[12] S. Maheshwari, M. Tsapatsis, F. S. Bates, *Macromolecules* **2007**, *40*, 6638–6646.

[13] a) F. C. Frank, J. S. Kasper, *Acta Crystallogr.* **1958**, *11*, 184–190; b) F. C. Frank, J. S. Kasper, *Acta Crystallogr.* **1959**, *12*, 483–499.

[14] a) X. Zeng, G. Ungar, Y. Liu, V. Percec, A. E. Dulcey, J. K. Hobbs, *Nature* **2004**, *428*, 157–160; b) S. Lee, M. J. Bluemle, F. S. Bates, *Science* **2010**, *330*, 349–353.

[15] a) J. M. Sullivan, in *Foams and emulsions*, Springer, Berlin, **1999**, pp. 379–402; b) Y. P. Yarmolyuk, P. Kripyakevich, *Sov. Phys. Crystallogr.* **1974**, *19*, 334–337.

[16] S. Lee, C. Leighton, F. S. Bates, *Proc. Natl. Acad. Sci. USA* **2014**, *111*, 17723–17731.

[17] G. M. Grason, B. A. DiDonna, R. D. Kamien, *Phys. Rev. Lett.* **2003**, *91*, 058304.

[18] N. Xie, W. Li, F. Qiu, A.-C. Shi, *ACS Macro Lett.* **2014**, *3*, 906–910.